



This is a repository copy of *Time-resolved yield stress measurement of evolving materials using a creeping sphere*.

White Rose Research Online URL for this paper:  
<http://eprints.whiterose.ac.uk/86459/>

Version: Accepted Version

---

**Article:**

Kashani, A., Provis, J.L., Van Deventer, B.B.G. et al. (2 more authors) (2015)  
Time-resolved yield stress measurement of evolving materials using a creeping sphere.  
Rheologica Acta. Published Online 4 February 2015. ISSN 0035-4511

<https://doi.org/10.1007/s00397-015-0839-x>

---

**Reuse**

Unless indicated otherwise, fulltext items are protected by copyright with all rights reserved. The copyright exception in section 29 of the Copyright, Designs and Patents Act 1988 allows the making of a single copy solely for the purpose of non-commercial research or private study within the limits of fair dealing. The publisher or other rights-holder may allow further reproduction and re-use of this version - refer to the White Rose Research Online record for this item. Where records identify the publisher as the copyright holder, users can verify any specific terms of use on the publisher's website.

**Takedown**

If you consider content in White Rose Research Online to be in breach of UK law, please notify us by emailing [eprints@whiterose.ac.uk](mailto:eprints@whiterose.ac.uk) including the URL of the record and the reason for the withdrawal request.



[eprints@whiterose.ac.uk](mailto:eprints@whiterose.ac.uk)  
<https://eprints.whiterose.ac.uk/>

# Time-resolved yield stress measurement of evolving materials using a creeping sphere

Alireza Kashani<sup>#</sup>, John L. Provis<sup>\*</sup>, Ben B.G. van Deventer<sup>†</sup>, Greg G. Qiao<sup>#</sup>, Jannie S.J. van Deventer<sup>#, †</sup>

<sup>#</sup>*Department of Chemical and Biomolecular Engineering, University of Melbourne, Victoria 3010, Australia*

<sup>\*</sup>*Department of Materials Science and Engineering, University of Sheffield, Sheffield S1 3JD, United Kingdom*

<sup>†</sup>*Zeobond Pty Ltd, P.O. Box 23450, Docklands, Victoria 8012, Australia*

Corresponding author: John L. Provis, Email: [j.provis@sheffield.ac.uk](mailto:j.provis@sheffield.ac.uk), Tel: +44 114 222 5490

**Abstract** Physico-chemical phenomena influenced by aging or reaction can result in rheological changes across several orders of magnitude, but the classical rheometry methods available for analysis of concentrated suspensions can face challenges in correctly measuring the yield stress of aging/reacting (evolving) materials and need some precautions to enable precise measurement of the evolution of the yield stress with time. Here, a creeping sphere method has been applied to measure time-resolved yield stress; the force required to pull a solid sphere at very low velocity is used to calculate yield stress using previous analytical solutions for local flow of a creeping sphere in yield stress materials. The measured yield stress values agree well with the data recorded using vane-in-cup geometry for time-independent measurements using Carbopol gel. The creeping sphere is less affected by shear history because of the constantly changing shear region, and therefore measures yield stress changes in evolving materials such as cement for a long time period in a single run, without altering ongoing structural network bond formation.

**Keywords** rheology, yield stress, creeping sphere, non-Newtonian Fluids, concentrated suspensions, cement

## Introduction

The rheological behavior of aging/reacting fluids can change noticeably as time passes. These changes have considerable impact on workability, transportation, and product quality in different applications such as mining, the food industry, and the design and use of construction materials. Time-resolved rheological changes are caused by various phenomena in different materials. For instance, in cements these changes are mainly the result of water-consuming reactions and the formation of reaction products which increase the paste yield stress by increasing inter-particle interactions (Gauffinet-Garrault 2012). Alkali-activated slag binders have been developed as a low-CO<sub>2</sub> alternative to Portland cement, but they are restricted in some areas of practice due to challenging rheology (Bernal and Provis 2014, Provis and Bernal 2014). It has been shown that yield stress increases dramatically after mixing for alkali-hydroxide-activated slag, but remains constant for alkali-silicate-activated slag, for 20 minutes after mixing using the vane in cup rheometry method (Kashani et al. 2014).

The slump test is the most popular test for measuring flowability of concretes and mortars. This test measures the retained height of a compacted inverted cone of concrete under the action of gravity. The slump test is a simple method which gives good indications of rheological behavior, related to yield stress and apparent viscosity. Changes in slump as a function of time after mixing of cement (termed 'slump loss') are used to calculate the pressure evolution associated with casting and to estimate sedimentation (Kovler and Roussel, 2011). The standardized basic slump test is applied to concrete and requires a large volume of material; a variety of 'mini-slump' tests have been proposed for paste and mortar mixes using smaller cones, but there is not yet any formal agreement on the optimal cone geometry or size for such a test.

The use of the vane method to measure the time-resolved yield stress of aging/reacting binders has some limitations. Accurate time-resolved yield stress measurement using the vane method requires repeated preparation of new samples because irreversible particle depletion close to the vane tips induces errors in the measurement and causes underestimation of the yield stress (Ovarlez et al. 2011). This repeated sample preparation is also subject to

reproducibility errors. It is common to use pre-shear hand-mixing before each measurement to avoid this problem, but this can still introduce errors when evolving materials are used because rheological behavior is affected by shear and agitation (Ovarlez et al. 2011).

Multiple sequential yield stress measurements using the same shear region in a single sample do not allow the material to undergo structural formation at rest, which would otherwise result in a yield stress increase. This structural breakdown by repeated measurements, or by premixing before each measurement, tends to be irreversible at higher shear stress for some non-Newtonian fluids (Gueslin et al. 2009). For reactive binders such as cement paste and alkali-activated slag, mixing and high shear forces cause breaking of agglomerates and manipulation of the process of reaction, which affect the rheological behavior (Williams et al. 1999, Yang and Jennings 1995), and this influence of mixing history on material properties can even be observed in the hardened-state properties of the material in some cases (Palacios and Puertas 2011). The study of the rheological behavior of cement paste using magnetic resonance imaging velocimetry has shown that rheology is influenced by partially reversible shear-induced structure deformation and irreversible structure formation due to hydration (Jarny et al. 2008). In addition, mixing of a very high yield stress material can cause heterogeneity by entrainment of air in the material.

Non-destructive methods such as ultrasound propagation have been used to monitor the early age changes in rheological properties induced by cement hydration, by examining the changes in shear wave reflection through Portland cement (Lootens et al. 2009, Müller et al. 1999, Voigt and Shah 2004). The evolution of the storage and loss shear moduli of cement paste as a function of time was related to cement hydration and product formation (Jupe et al, 2012). Mixing-free methods with continually changing shear regions such as penetrometry (Amziane and Ferraris 2007, Bernal et al. 2011, Lootens et al. 2009, Sant et al. 2008) have also been introduced to measure the time-resolved yield stress of evolving cementitious materials.

One experimental penetrometry method is the Vicat needle test, ASTM C191 (ASTM International 2013) which is widely used to assess solidification processes, especially in cementitious materials. This method measures the penetration distance of a flat-headed

needle inserted from the material surface under a constant force, where 'setting' is defined in terms of the development of a resistance to penetration by the needle. However, this method is only applicable to semi-solid materials showing minimum shear yield stress of 20 kPa (Sant et al. 2008), and does not give any information regarding rheological behavior in the fluid state. In a study by Lootens et al. (Lootens et al. 2009), cement paste yield stress was measured during setting using a penetration test method. They used a hemispherical tip mounted on a rod, and the drag force on the tip during penetration at a velocity of 1  $\mu\text{m/s}$  was associated with yield stress by assuming of quasi-static flow in a Bingham fluid.

Flow around a rigid sphere has been studied in non-Newtonian fluids which can be described by the Bingham plastic (Beris et al. 1985, Blackery and Mitsoulis 1997) and Herschel–Bulkley (H–B) models (Atapattu et al. 1995, Beaulne and Mitsoulis 1997), as well as other yield stress materials (Gueslin et al. 2006, Gueslin et al. 2009, Tabuteau et al. 2007), and these studies have provided both experimental data and numerical simulations for flow behavior, drag forces, and shear regions around the sphere. A practical method which measures rheological behavior based on the movement of a sphere is known as the ball measuring system (BMS), which was introduced by Müller et al. (Müller et al. 1999). In this method an eccentrically rotating solid sphere fixed to a thin holder is dragged within a body of fluid sufficiently large to approximate an infinite medium, following a circular path. However, this method has shown some challenges in geometry and design (Schatzmann et al. 2009).

In this study, a new method is proposed to measure yield stress by pulling a sphere vertically at very low and constant velocity through evolving materials. Yield stress is calculated from the measured force data based on equations published in previous numerical and experimental studies of rigid sphere motion (Atapattu et al. 1995, Beaulne and Mitsoulis 1997, Beris et al. 1985, Blackery and Mitsoulis 1997, Schatzmann et al. 2009, Tabuteau et al. 2007). The calculated yield stress values are also compared with data from the vane in cup method using a Carbopol gel which shows time-independent rheological behavior. The effects of sphere size, roughness, and velocity on the measured yield stress were studied. The creeping sphere method is then adopted to measure the time-resolved changes in yield stress

of evolving cementitious materials, which enables a long-duration yield stress measurement in a single run without interfering with the shear history of the material.

## Experimental details

### *Materials*

Carbopol Ultrez 10 polymer powder was provided by Lubrizol, China. It was slowly added into water (0.3 wt.%) while mixing at 1000 rpm for 20 minutes, then 5M NaOH solution (NaOH pellets, AR grade, Sigma-Aldrich, Australia, dissolved in milli-Q grade water) was added dropwise until reaching a pH of 6 to initiate gelation. The Carbopol gel was allowed to rest for 24 hours in order to develop a homogenous structure. Ground granulated blast furnace slag (GGBFS) and anhydrous sodium metasilicate ( $\text{Na}_2\text{SiO}_3$ ) were provided by Zeobond Pty. Ltd., Australia. Ordinary Portland cement (OPC), Type GP (general purpose) according to AS3972 (Standards Australia 2010), was obtained from a local retailer. Rheobuild 1000 (BASF, Australia) as a cement plasticizer was used in one of the Portland cement samples at 1 wt. % of dry powder mass. After hand mixing of the powdered solids with water at a water/solids mass ratio of 0.45 in each case, the paste was mechanically mixed for 10 minutes at 500 rpm before yield stress measurement. Sodium silicate activated slag pastes were formulated with 0.225 and 0.45 mmol  $\text{Na}_2\text{O}$  per gram of slag, corresponding to the conditions used in previous work (Kashani et al. 2014).

### *Creeping sphere test setup*

Lead spheres of different diameters (shown in Table 1), sold commercially as fishing sinkers, were attached to an Instron microtester 5848 (Instron, USA) via a thin stainless steel rod. The force required to move the sphere at a very low, constant velocity (9.58 mm/min) is recorded by the Instron instrument. The selected velocity equals to the linear velocity of the tips of the vane H while rotating at 0.2 rpm (Section 2.3). The test setup is shown in Figure 1. The instrument was calibrated to zero force before each measurement. The sphere was located above the sample surface at the start of each experiment, then moved downward into the

sample. The force on the sphere was recorded until it reached about 20 mm above the bottom of the container. After resting for 15 minutes, it was pulled backward to the start point at the same velocity. After resting and before moving upward, the balanced force was manually set at zero. In this experiment the measured force during upward and downward movements is treated separately in order to calculate yield stress and for this reason the force before movement in each direction was set at zero. The detectable force range was from 0.001 to 5 N with a precision of 0.001 N. The force was measured at intervals of 0.1 s.

The buoyancy force (Equation 1) on the sphere in the Carbopol gel was also calculated with the assumption that the displaced volume of the gel,  $V$ , by insertion of the spheres is equal to the sphere volume ( $\rho_{gel}$ :  $1000 \text{ kg/m}^3$ ). The results are shown in Table 1.

$$F_B = Vg\rho_{gel} \quad (1)$$

**Table 1** Spheres and thin rod average diameters compared to the sample container diameter (120 mm)

Object	Average diameter (mm)	Ratio of container diameter to object diameter	Buoyancy force (mN)
Rod	1.47	83.74	<1
S8	8.49	14.15	2.85
S12	12.3	9.75	6.54
S18	18.35	6.54	30.31



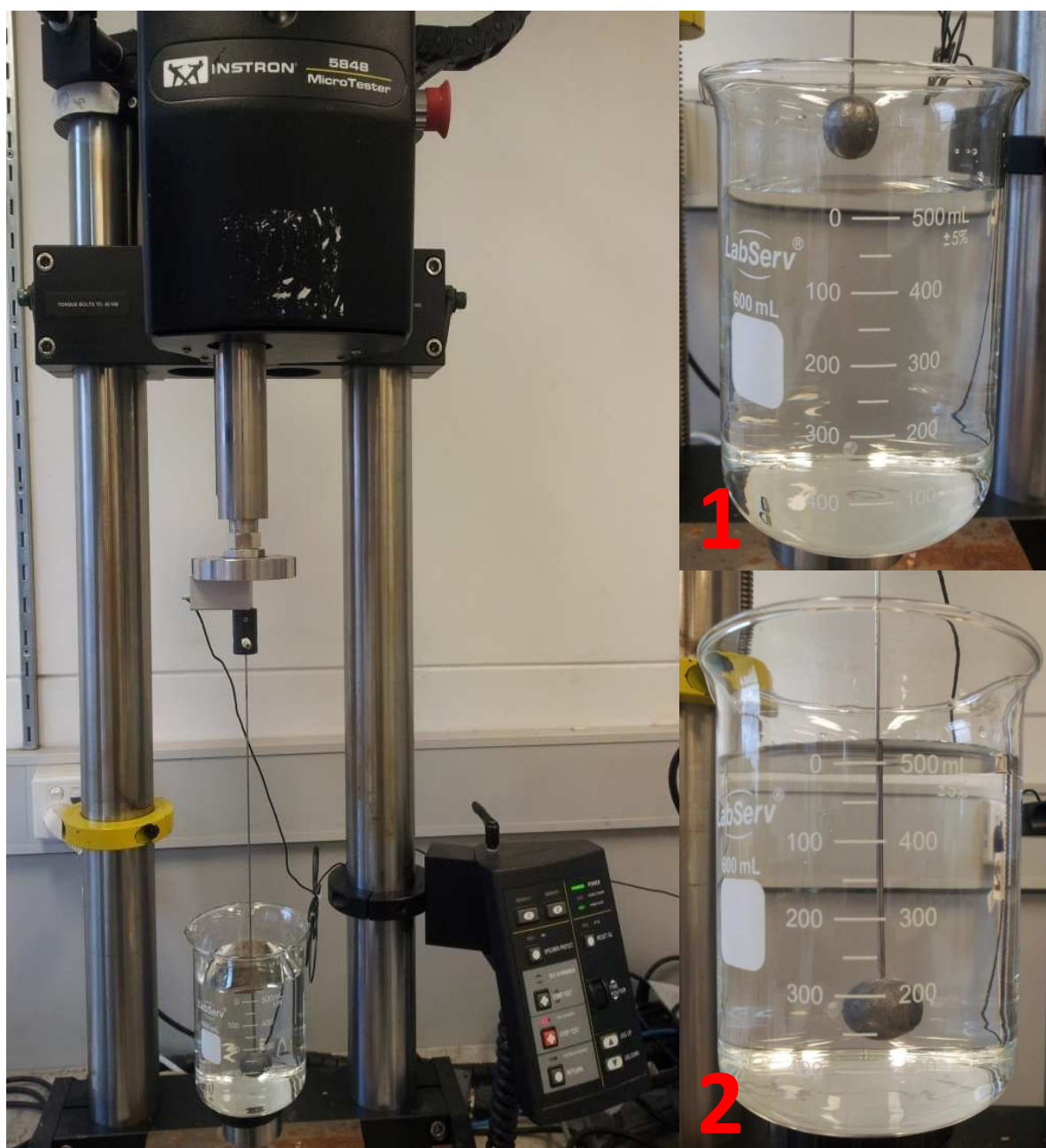


**Figure 1** Creeping sphere test using Instron microtester; the force is measured during movement of the sphere from 1 to 2 (downward movement) and then 2 to 1 (upward movement). The medium is water in the photograph

#### *Rheological test by the vane method*

The yield stress of samples was also measured using a Haake VT550 rheometer with vane H (a four-blade vane with length of 50.1 mm and diameter of 15.3 mm), in a sample volume



sufficient to simulate an infinite medium (Nguyen and Boger 1992). A direct yield stress measurement at a low rotational rate (0.2 rpm) was used because of the accuracy and reproducibility of the measured data (Nguyen and Boger 1985). Before each measurement the sample was mixed by hand to provide a homogenous paste, then let to rest for 30 seconds to dissipate residual stresses because of mixing, and afterwards the 0.2 rpm rotational rate was applied, corresponding to the methodology used in previous work (Kashani et al. 2014). The flow curve was also determined similarly by increasing the rotational rate in 8 consecutive steps from 2 rpm to 500 rpm with 30 seconds rest in between measurements, then the measured torque was related to shear stress according to Nguyen and Boger (Nguyen and Boger 1983). Shear rates at each shear stress was calculated based on a linear regression between the logarithm of shear stress and logarithm of angular velocity according to Nguyen and Boger (Nguyen and Boger 1987).

## Results and discussion

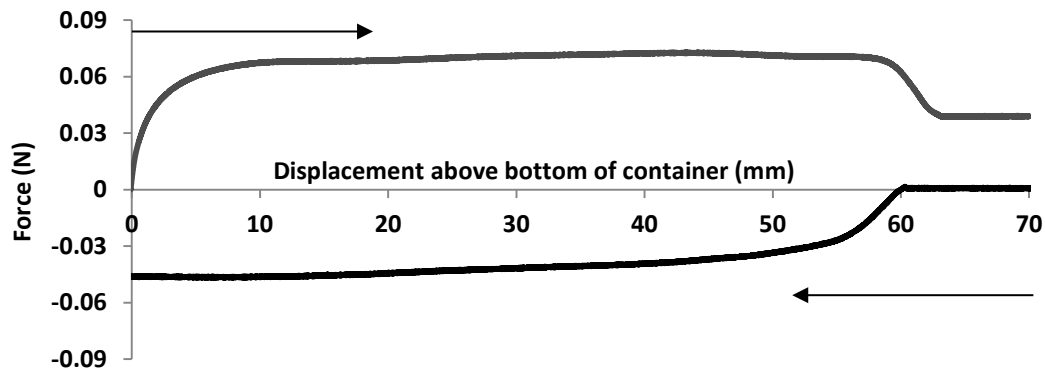
### *Force measurement of creeping sphere*

Figure 2 shows the force changes corresponding to the movement of the 8 mm lead sphere (S8) at a constant velocity of 9.58 mm/min in the Carbopol gel during downward (negative force as shown in Figure 2) and then upward movement (shown as positive force). The first noticeable force change starts when the sphere touches the sample surface during downward movement (shown as 60 mm displacement in Figure 2). At this point, the magnitude of the force on the sphere increases sharply until the sphere is completely below the gel surface. Similar behavior has been recorded for various objects becoming immersed in a yield stress fluid (Boujlel and Coussot 2012, Lootens et al. 2009); in this case, there is not an evident skin or surface tension effect in the initial stages of immersion.

Once the sphere is submerged, the force increases gradually during downwards motion until the sphere reaches the designated point close to the bottom of the container, which is shown as zero displacement in Figure 2. As soon as the sphere stops, the absolute force on the sphere suddenly decreases by removing the material resistance force against the movement

(not shown). During upward movement the force increases until the sphere moves steadily. As soon as the sphere breaks through the gel surface the force magnitude decreases until the sphere leaves the material. At this point the balanced force on the sphere would be zero if the force was not manually set at zero after the rest time (see Section 2.2).

Forces acting on the moving sphere within the gel are resistance to deformation from the gel, gravity, and buoyancy forces. The buoyancy force, compared to the measured force in Figure 2, is negligible (Table 1). The balanced force on the hung-in-air sphere was set at zero in order to eliminate the gravity force on the sphere. Therefore, the material resistance is assumed to be the sole reason for the force changes during sphere movement.



**Figure 2** Force vs. displacement for the lead sphere (S8) during downward ( $\leftarrow$ ) and upward movement ( $\rightarrow$ ) within the Carbopol gel at the velocity of 9.58 mm/min

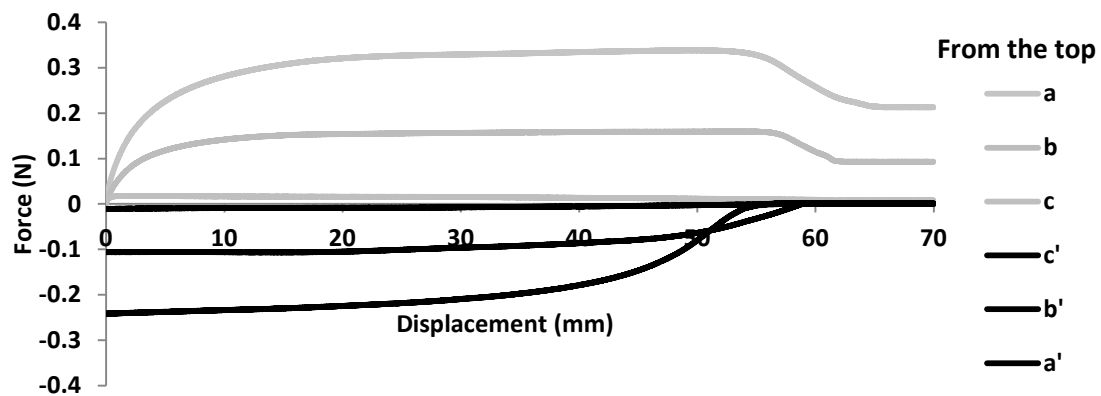


**Figure 3** Force vs. displacement for S18 (a, a'), S12 (b, b'), and the thin rod (c, c') within the Carbopol gel at the velocity of 9.58 mm/min (upward and downward movements are shown by grey and black lines, respectively)

The other two spheres of different sizes (S12 and S18), and also the same thin rod without any sphere attached (the dimensions are shown in Table 1), were used in similar experiments in the same Carbopol gel as depicted in Figure 3. The spheres with different diameters follow similar trends although the magnitude of the force and the point of the transition to the steady state condition are different, which is expected because of different volumes and surface areas of the spheres.

The force changes by movement of the rod are negligible as shown in Figure 3; only when a substantial length of the rod moves within the sample, a small force change is observed. Therefore the force change versus displacement is not sufficient to induce any interruption when it is attached to the spheres. Also, in order to have an effective force change caused by the rod, it first needs to have contact with the gel, however, it was observed that after insertion of the sphere into the gel, the rod was only partially covered at the top of the sphere (about the sphere diameter), and the remainder was contact-free during the movement of the sphere. The gap generated within the gel by insertion of the sphere was not fully recovered to fill around the rod. This situation was observed in both upward and downward movements and also for all other highly viscous samples used here. The gap was generated in the downward movement but recovered itself as the sphere was being pulled upwards. In both situations the amount of sample surrounding the top of the sphere was about a length similar to the sphere diameter, therefore, no concerns about the pseudo-infinite nature of the medium is presented (this will be discussed later, in section 3.3). The ability of the material to re-fill this gap depends on the sphere diameter and the yield stress of the medium, and in this case where a high yield stress gel was used, recovery did not fully occur. A similar observation was recorded in a high yield stress material using a penetrometry method (Lootens et al. 2009). However, if a low yield stress material is used, the situation would be different and the yield stress calculation must include the shear forces around the rod, which are neglected in the discussion and calculations for the sphere system here.

#### *Yield stress calculation by the creeping sphere method*

The free-fall of a solid sphere through a Bingham plastic fluid results in formation of a small envelope of sheared fluid around the sphere, the shape of which depends on the yield stress of

the fluid (Beris et al. 1985). There is also the possibility of some un-sheared regions forming as caps at the top and the bottom of the sphere, and potentially also some islands around the sphere, because of the appearance of flow stagnation points, depending on the dimensionless Bingham and yield stress numbers (Beaulne and Mitsoulis 1997). This has been shown by analytical and numerical studies of sphere motion in Bingham plastic (Beris et al. 1985, Blackery and Mitsoulis 1997) and H-B fluids (Atapattu et al. 1995, Beaulne and Mitsoulis 1997). Regardless of flow behavior models (Bingham, H-B, or any other models), the assumptions around the yield stress are common. It would intuitively be expected that the shear envelope around a sphere should be axisymmetric although small deviations have recently been observed using flow imaging because of interference of an upward fluid motion in the wake path of the sphere (Gueslin et al. 2006, Gueslin et al. 2009).

The numerical studies of Beris et al. (Beris et al. 1985) showed a critical dimensionless yield stress,  $Y_g = 0.143$  (Equation 2), above which a solid sphere cannot move within a yield stress material and the medium acts as a solid. This critical yield stress value was obtained by mesh refinement of the shear regions around the creeping sphere at very low Reynolds number ( $Re \ll 1$ ) and integral calculations of the maximum and minimum variation principles (Beris et al. 1985). This critical yield stress value has been confirmed by several other numerical and experimental studies (Beaulne and Mitsoulis 1997, Blackery and Mitsoulis 1997, Schatzmann et al. 2009, Tabuteau et al. 2007).

$$Y_g = 2\tau_y \pi R^2 / F \quad (2)$$

$Y_g$ : dimensionless yield stress

$F$ : externally applied force (N)

$R$ : sphere radius (m)

$\tau_y$ : yield stress (Pa)

Therefore, the minimum external force required to move a sphere within a yield stress material is when  $Y_g = 0.143$ . This minimum force is then associated with the yield stress in Equation 2. In order to determine this minimum force, first the movement velocity needs to be low enough in order to minimize inertial effects. This force also needs to be constant regardless of the sphere location as far as it is fully covered by an infinite medium and moves

steadily (steady-state condition). This situation is observed in the upward movement when the force increases to a constant value and is maintained until the sphere approaches the medium surface.

During the downward movement a steady-state condition with constant force was not achieved. Significant entrainment of air was observed as the sphere penetrated the surface of the gel. The entrained air evolved from a cylindrical column to a conical shape, and ultimately separated from the surface of the sphere. The evolution of the entrained air has the effect of gradually increasing the proportion of the sphere that is exposed to the gel medium, hence and a gradual increase in force. This phenomenon is absent in the equivalent the upward motion of the sphere major. Thus it is expected that air entrainment is the primary reason that an equilibrium state was not observed for the downward penetration.

If the plateau in the force during the upward movement of different spheres in Figure 3 is used as the minimum force, then Equation 2 gives the yield stress of the Carbopol gel considering  $Y_g = 0.143$ . The results are compared with the yield stress measured for the same gel by the Haake rheometer using vane H, in Figure 4. The yield stress measured by this method agrees well with the data recorded by the vane method for the time-independent measurements.

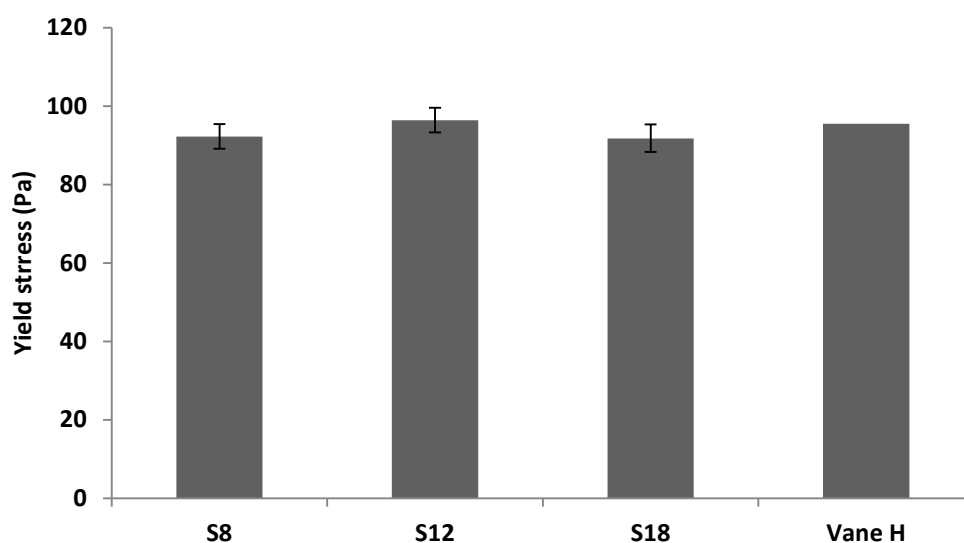


**Figure 4** Yield stress of the Carbopol gel using creeping sphere with different sizes compared to the measured data of the same sample using vane H (error bars are due to out of roundness of the lead spheres)

Provision of an infinite medium for sphere movement is of great importance to eliminate the container wall effects which cause shear region deformation. For the vane method, double the size of the vane diameter and length is considered to be the minimum container size required to avoid rigid wall effects (Nguyen and Boger 1983). For a sphere moving in a cylinder of a Bingham plastic material, Blackery and Mitsoulis (Blackery and Mitsoulis 1997) found that close to a dimensionless yield stress of 0.143, a range of 2:1 to 50:1 ratios of cylinder diameter to sphere diameter did not cause any difference in representation of an infinite medium. Table 1 shows that the ratio of the container diameter to the sphere diameter, for the different spheres used in this study, is clearly sufficient to represent an infinite medium, and this is confirmed by the similar yield stress results for the three sphere sizes in Figure 4.

#### *Effects of rest time, velocity, and surface roughness on yield stress measurements*

The previous section showed that a single yield stress measurement using the creeping sphere method produced comparable results to the vane in cup method for Carbopol gel. However, the key aim of using the creeping sphere method is to study time-resolved yield stress for aging or reacting materials such as cementitious binders. As discussed above, the vane method is subjected to errors when the yield stress test is run repeatedly for a single sample over time. Here it is shown that such a problem does not occur for the creeping sphere method, as the shear region continually changes. Therefore, this method is capable of measuring yield stress over longer time periods, which also allows the material to rest between measurements without interference from external shear forces caused by mixing between consecutive runs.

As was mentioned above, the plateau force during the upward movement of the sphere was used to calculate yield stress. Carbopol gel is known to have negligible time-induced rheological behavior (Boujlel and Coussot 2012, Tabuteau et al. 2007), which means that yield stress is constant as time passes. Therefore, after reaching the plateau force in upward movement, if the sphere stops and rests for several minutes, then the force must reach the same value when movement is re-started. As shown in Figure 5, after stopping the movement

the force drops suddenly, and as soon as the test is restarted, it returns to the previous plateau level.

A similar test in the vane method produced quite similar results for Carbopol gel. Figure 6 shows the measured torque against the displacement of the vane tip in its circular path at the rotational rate of 0.2 rpm. After reaching the maximum torque, which is used to calculate the yield stress, the torque is constant while the vane is rotating. As soon as the vane stops, the measured torque drops but reaches the same value when it starts to rotate again after 15 minutes rest. The only difference here is that the vane rotates in the same path several times, but the shear region of the creeping sphere is constantly changing. This is an advantage to measure yield stress in a fresh section of the material which is less affected by shear history, especially for evolving and reacting binders although for a simple yield stress material such as Carbopol gel the difference between these two methods seems to be negligible when Figures 5 and 6 are compared. Therefore, changes in yield stress induced by structure formation of the evolving material can be studied over an extended period by making several stops during a single upward movement. Because of the continually changing shear regions, a fresh section of the material is tested each time in the creeping sphere method.

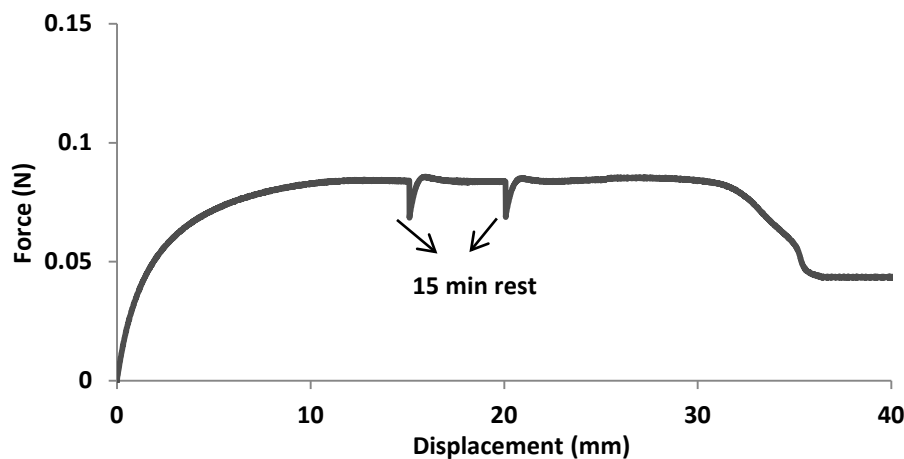


**Figure 5** Two sets of rests each for 15 minutes during the upward movement of sphere S8 within Carbopol gel at a velocity of 9.58 mm/min



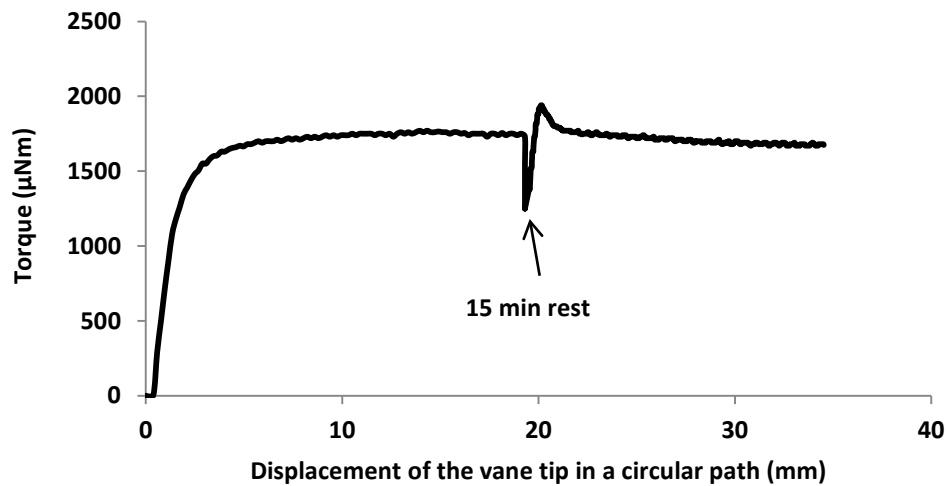


**Figure 6** The measured torque of Carbopol gel against the displacement of the vane tip in its circular path at 0.2 rpm with 15 min stop between two consecutive measurements

In conducting measurements with this technique, the sphere velocity must be low enough to minimize inertial effects. This is also the case in direct yield stress measurement by the vane in cup method (Nguyen and Boger 1985), where a very low rotational rate ( $\leq 0.2$  rpm) is used to measure the yield stress. Here, the maximum sphere velocity was set equal to the linear velocity of the tips of the vane H while rotating at 0.2 rpm, which is 9.58 mm/min. Velocities of 2 and 5 mm/min were also applied in the same system, to evaluate the effect of different velocities on yield stress measurement. The results for sphere S18 at these velocities are shown in Figure 7, for upward movement through Carbopol gel, and it is clear that as long as the velocity is low enough to exclude inertial effects, the results obtained are the same. This is in agreement with previous studies of low velocity sphere motion in yield stress materials, which have shown that the steady-state drag force is dominated by the yield stress rather than sphere velocity (Chafe and de Bruyn 2005, Jossic and Magnin 2001, Zhu et al. 2001) and direct yield stress measurement using different rotational rates of the vane (Nguyen and Boger 1983).

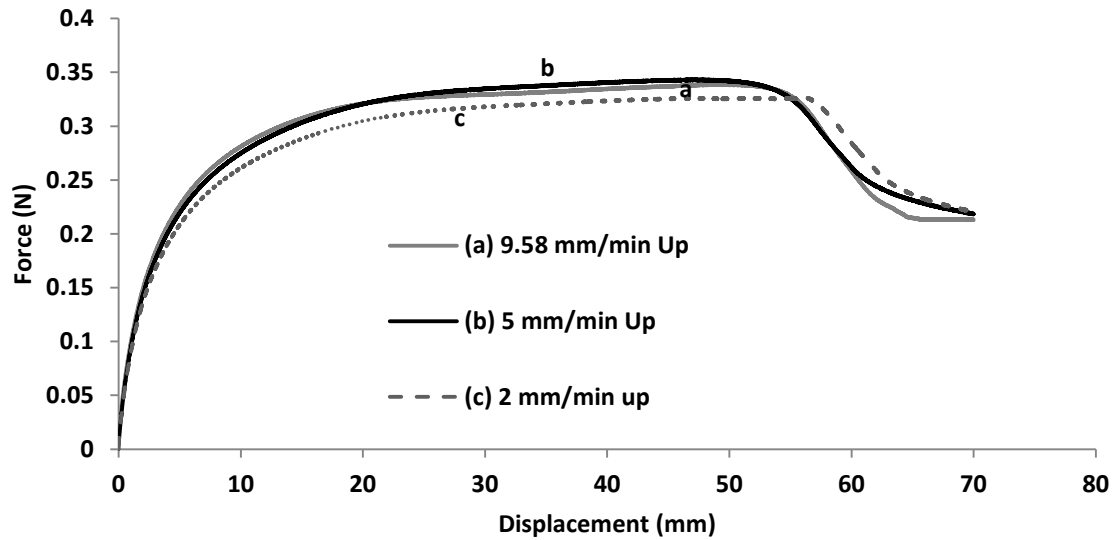


**Figure 7** Force vs. displacement during upward movement of the S18 sphere within Carbopol gel at velocities of 9.58, 5, and 2 mm/min

The flow around the sphere must clearly have a very low Reynolds number ( $Re \ll 1$ ) in order to associate resistance force with yield stress. Reynolds number calculation for non-Newtonian fluids requires evaluation of flow behavior by fitting of flow curves to a fitting model such as the H-B model in order to use the flow exponents in Reynolds number calculation. The generalized Reynolds number for a sphere moving in an H-B fluid (Beaulne and Mitsoulis 1997) is shown in Equation 3. The flow curve of the Carbopol gel is shown in Figure 8, and fits to the H-B model ( $n = 0.3$  and  $k = 52.47 \text{ Pa.s}^n$ ). For the 9.58 mm/min velocity used here, the Reynolds number is  $1.6 \times 10^{-6}$ , which is within the requirement of creeping flow without any involvement of inertia.

$$Re^* = \frac{V^{2-n} D^n \rho}{k} \quad (3)$$

*Re*: Reynolds number for sphere in H-B fluid

*V*: sphere velocity (m/s)

*D*: sphere diameter (m)

$\rho$ : Carbopol gel density ( $\text{kg/m}^3$ )

*n*: flow index in H-B fluid model

*k*: consistency factor in H-B fluid model ( $\text{Pa.s}^n$ )

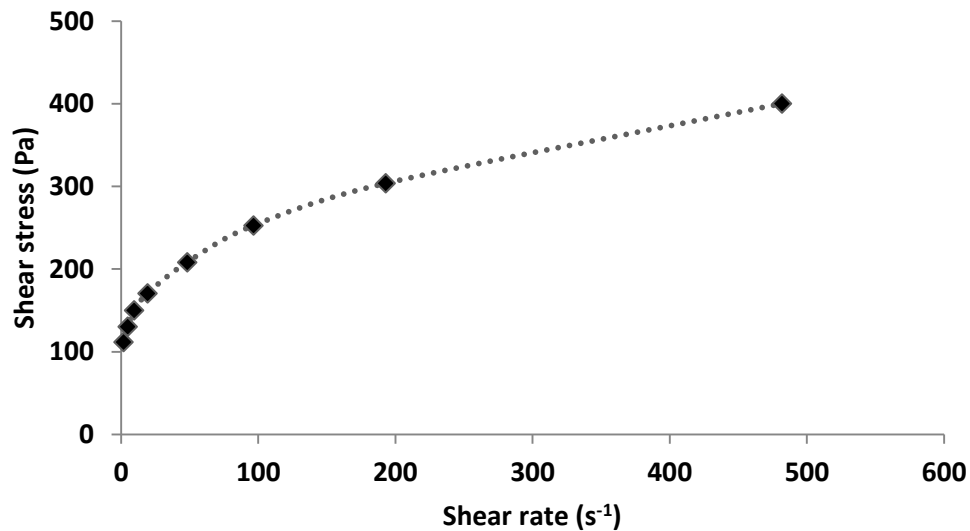


**Figure 8** The flow curve of the Carbopol gel which fits to the Herschel–Bulkley model (dashed line)

Another phenomenon which could affect the measured force, and hence lead to underestimation of the yield stress, is sphere slip during movement within the medium. Based on the absence of a decrease in force during measurement, a no slip condition has been assumed here. In other words, if during the movement of the sphere the material slipped at its surface, then the sphere could move freely with negligible force detected. In such situations the force might decrease to near zero values, however this was not observed. In the case of a slip condition, different sphere diameters would have led to variation of yield stress due to a differing slip extent, however this was also not experienced.

Moreover, the lead spheres employed in this work have very rough surfaces (Figure 9) that minimize any possibility of slippage of the gel/paste on the surface. An experiment was conducted to evaluate the effect of roughness on yield stress calculation by coating a layer of paint having fine sand particles on S12 sphere as shown in Figure 9. This provides a roughness of about few hundred micrometers. The calculated yield stress results in Figure 10 shows that surface roughness has a negligible effect on yield stress. This is in accordance with Tabuteau et al. (Tabuteau et al. 2007) who found the effects of roughness to be negligible on measured drag force of creeping sphere in Carbopol gel.

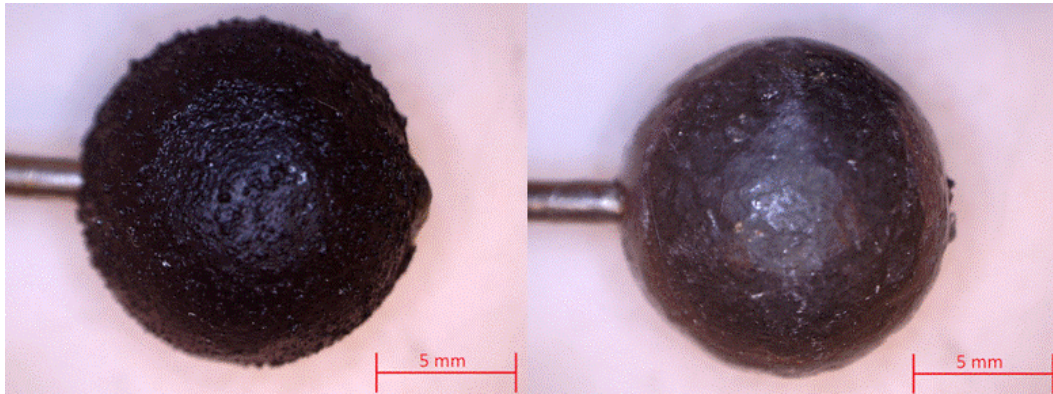


**Figure 9** A comparison between surface roughness of original S12 sphere (right;  $d_{ave}$ : 12.3 mm) and sand-coated S12 sphere (left;  $d_{ave}$ : 12.4 mm)

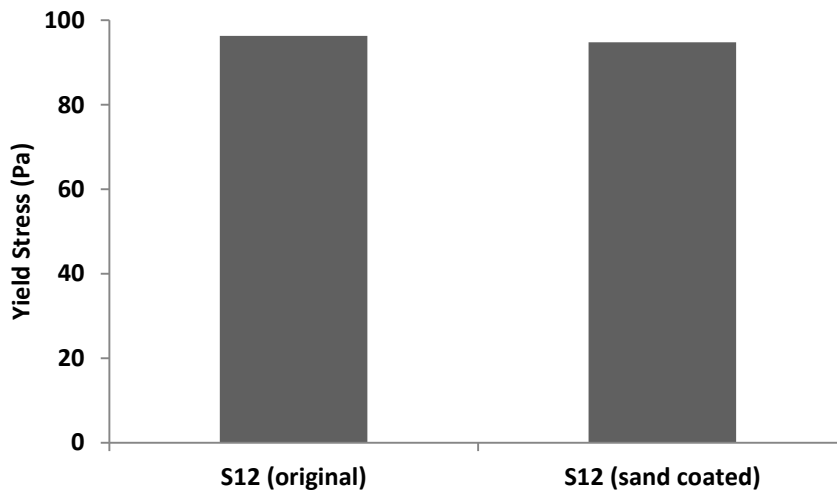


**Figure 10** Effect of roughness on yield stress measurement of Carbopol gel using the S12 spheres shown in Figure 9.

A different approach in order to calculate yield stress from force measurement was used by Lootens et al. (Lootens et al. 2009) who studied cement paste yield stress during setting using a penetration test method. They used a half sphere tip mounted on a rod, and the drag force on the tip during penetration at low velocity was associated with yield stress. They assumed Stokes' law in a Bingham fluid and a direct relationship was then developed between Stokes drag force and yield stress by exclusion of plastic viscosity because of the very low velocity of  $1 \mu\text{m/s}$ , which provides a quasi-static condition. Whilst in this study the very low Reynolds number supports the creeping flow assumption, the lowest velocity is much higher than the  $1 \mu\text{m/s}$  required to justify the assumption of quasi-static flow. Furthermore, the Carbopol gel

used here does not follow the Bingham model. Therefore, considerable differences in velocity and flow behavior do not allow use of the same yield stress calculation in our model system.

### *Measuring time-resolved yield stress of evolving cementitious binders*

The same method as used in section 3.2 to measure the yield stress of the Carbopol gel was also applied to Portland cement-water and ground granulated blast furnace slag-water pastes, and sodium silicate activated slag at dosages of 0.225 and 0.45 mmol Na<sub>2</sub>O/g slag. In contrast to the observations for the Carbopol gel, after resting in these reacting systems the force increases substantially, as seen in Figure 11 for the example of the slag-water paste. Even for this paste, which is considered a very slowly reacting binder (Chen and Brouwers 2007), the structural formation at rest is the process of re-agglomeration of formerly dispersed particles because of their high affinity and sometimes by formation of the products between dispersed particles and on their surface. This re-agglomeration of particles will increase particle-particle interaction, hence yield stress.

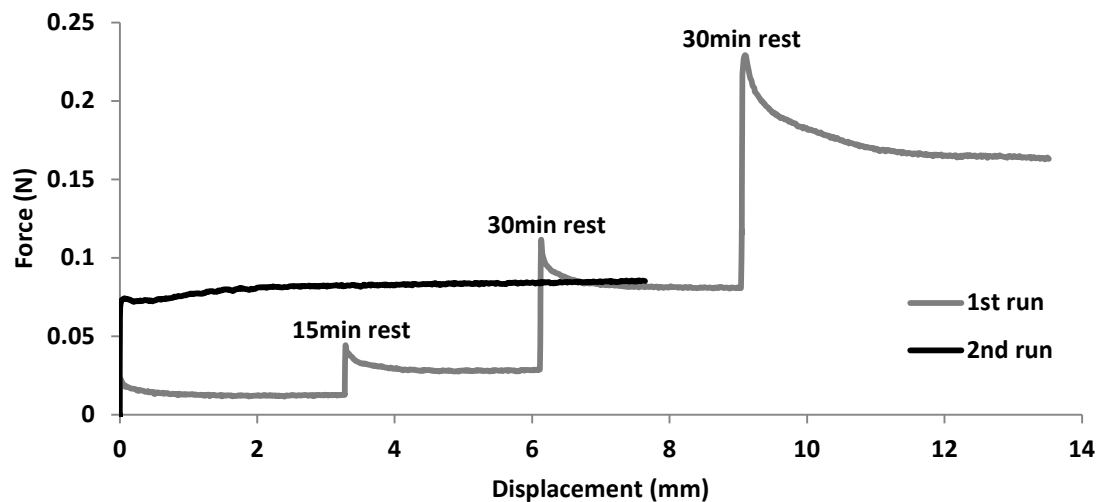


**Figure 11** Force vs. displacement of slag paste at two consecutive runs using sphere S8: the first run with 15, 30, and 30 min rest during upward movement, and the second run immediately started after the first run with hand mixing in between.

However, Figure 11 shows that the yield stress increase as a result of structural bond formation at rest is partially reversible by external shear forces. When the same slag-water paste was used for the second run of the yield stress measurement after hand mixing, lower

yield stress was recorded compared to the value that had been reached at the end of the first run. This clearly shows that any method requiring pre-mixing between repeated measurements is incapable of monitoring actual yield stress increase caused by structural bond formation at rest. Conversely, the creeping sphere method is a simple and powerful solution to monitor time-resolved yield stress changes of such materials.

Figure 12 shows the time-resolved yield stress changes measured in different cementitious binders. The time measurement starts as soon as water is added to the solid powders, and considering the mixing, downward movement, and rest time, the recording of data during upward movement commences 40 minutes after the start of mixing. The yield stress values measured for highly reactive binders such as cement paste and alkali-activated slag with higher activator dosage increase rapidly as time passes. This is attributed to water-consuming reactions and formation of the products causing formation of a three dimensional structure which increases the inter-particle forces hence yield stress (Figura and Prud'homme 2010, Gauffinet-Garrault 2012, Jarny et al. 2008, Palacios et al. 2008, Sant et al. 2008).

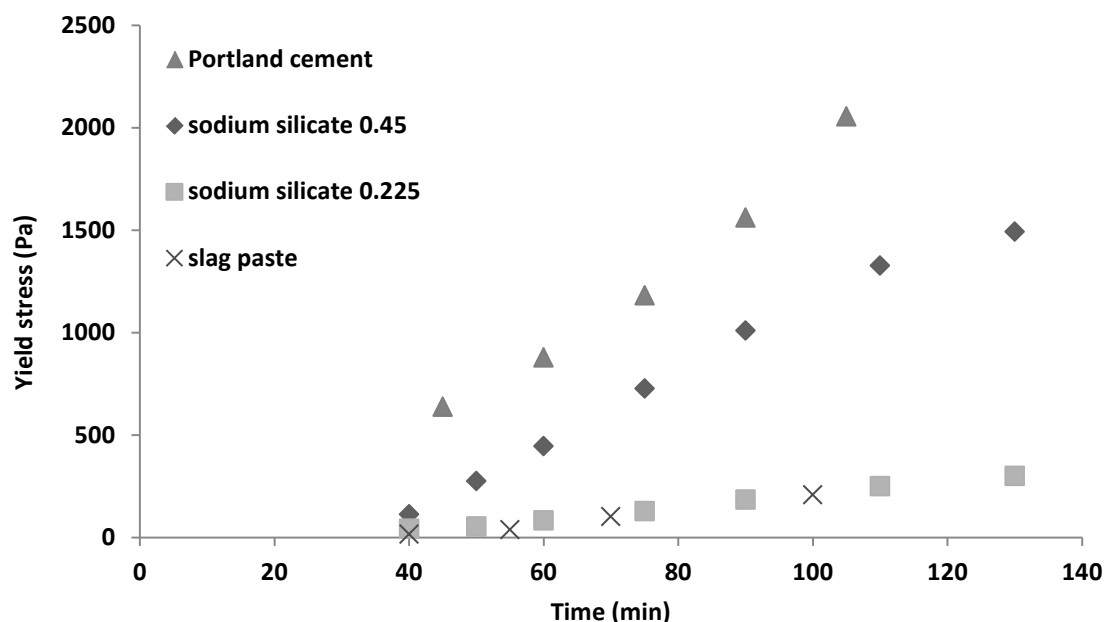


**Figure 12** Time-resolved yield stress of slag and Portland cement paste and sodium silicate activated slag at 0.225 and 0.45 mmol Na<sub>2</sub>O/g slag measured using the creeping sphere method

However, when a plasticizer with some retarding effect has been used at the same water to solid ratio for Portland cement, the yield stress changes were insignificant in the same time

period (Figure 13). This is due to the de-flocculation and de-agglomeration effects of the plasticizer which reduce the inter-particle forces and prevent reformation of structural bonds. This could also retard hydration reactions and the formation of solid products, which will slow the yield stress increase (Flatt and Schober 2012, Hanehara and Yamada 1999).

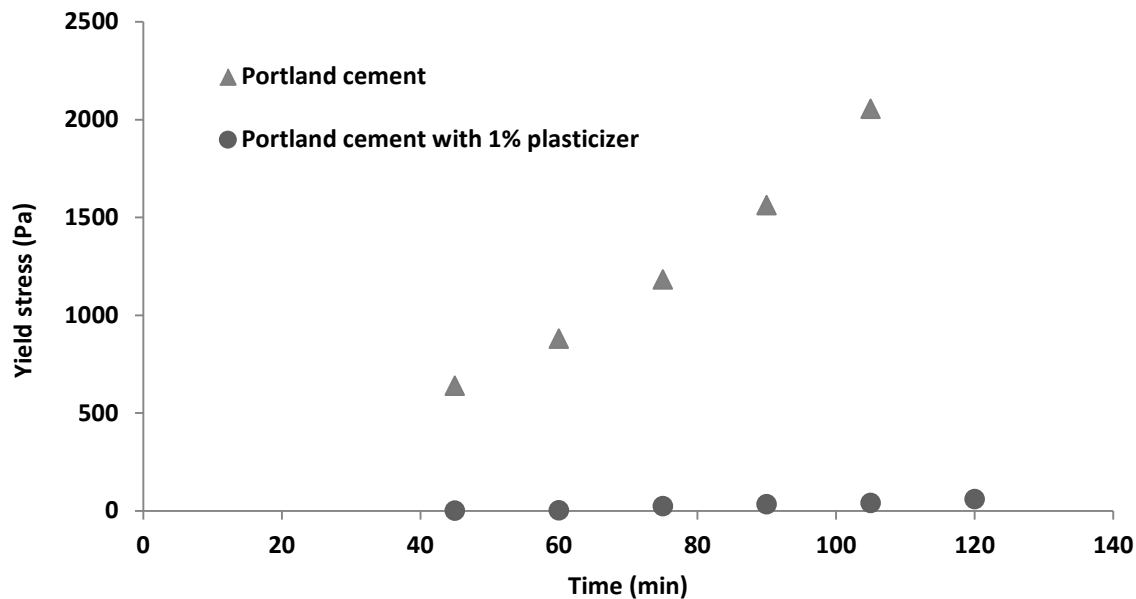


**Figure 13** Time-resolved yield stress of Portland cement paste and its counterpart with 1 wt. % plasticizer based on dry mix (w/s: 0.45)

In cement, calcium silicate hydrate (C-S-H) as the main hydration product precipitates on the surface of un-reacted particles and causes aggregation of the particles into grains. Then inter-particle forces will increase not just because of greater forces between C-S-H layers but also due to an increase in surface area of the particles (Gauffinet-Garrault 2012), although the roles of ettringite phases could be equally important at the early age of cement hydration because of rapid formation of these products and their roles in adsorption of chemical plasticizers (Plank and Hirsch 2007, Rossler et al. 2008, Zingg et al. 2008). Calcium (sodium) aluminosilicate hydrate as the main product of alkali-activated slag could behave similarly although it has not yet been studied in sufficient detail. However, the reaction products firstly form in pore solution regions in alkali- activated slag, where there is a high concentration of soluble silicates, compared to OPC where the C-S-H precipitates mainly on cement particles, therefore water consumption and dissolution with the formation of the products into the solution produce a network between slag particles which seems more dominant in alkali-



activated slag (Richardson 1999, Wang and Scrivener 1995). This cohesive network will increase inter-particle forces and hence yield stress if it is not disturbed by external shear forces such as mixing.

Yield stress measurement versus time of alkali-activated slag using the vane in cup method and hand-mixing between consecutive measurements in a previous study (Kashani et al. 2014) showed no yield stress increases for slag paste and sodium silicate-activated slag at similar dosages up to 20 minutes. However, the creeping sphere method proved that structural bond formation in these binders happens during resting which increases the yield stress. Nevertheless, it is believed that time-induced structural network bonds formation seems to be overshadowed by the external shear forces during hand-mixing when repetitive yield stress measurements are conducted by the vane method.

## Conclusions

This paper has introduced a new method of measuring yield stress based on local flow around a creeping sphere. The minimum external force to pull a solid sphere within a non-Newtonian fluid is associated with the yield stress by using a dimensionless yield stress value of  $Y_g = 0.143$  which defines the transition point between stagnation and local flow of a solid sphere within a yield stress material. The yield stress measured by this method agrees well with the data recorded by the vane in cup geometry for time-independent measurements. The effects of different sphere sizes and velocity on the measured yield stress are negligible, as long as the creeping flow regime is maintained. The container size diameter, which was more than six times the diameter of the sphere in the tests presented here, is sufficient to show no wall effect. No slip around the sphere during the movements was experienced.

The creeping sphere method was also applied to measure the time-resolved yield stress of evolving cementitious binders. Pausing the sphere motion while moving in a single path enables a long time period of yield stress measurement. Also, any interference caused by external shear forces or shear history is minimized, and continually changing shear regions

provide a fresh medium for every measurement. This method is capable of monitoring yield stress increase caused by structural bond formation in particulate suspensions at rest.

## Acknowledgements

This work has been funded through an Australian Research Council Linkage Project grant, co-funded by Zeobond Pty. Ltd., and also benefited from support through the Particulate Fluids Processing Centre, a Special Research Centre of the Australian Research Council. The authors also want to thank Mr. Andrew Alchin from Bronson & Jacobs (Sydney) for supplying Carbopol samples.

## References

- Amziane S, Ferraris CF (2007) Cementitious paste setting using rheological and pressure measurements. *ACI Mater J* 104: 137-145
- ASTM International (2013) Standard test method for time of setting of hydraulic cement by Vicat needle, ASTM C191-13, West Conshohocken, PA
- Atapattu DD, Chhabra RP, Uhlherr PHT (1995) Creeping sphere motion in Herschel-Bulkley fluids: flow field and drag. *J Non-Newtonian Fluid Mech* 59: 245-265
- Beaulne M, Mitsoulis E (1997) Creeping motion of a sphere in tubes filled with Herschel-Bulkley fluids. *J Non-Newtonian Fluid Mech* 72: 55-71
- Beris AN, Tsamopoulos JA, Armstrong RC, Brown RA (1985) Creeping motion of a sphere through a Bingham plastic. *J Fluid Mech* 158: 219-244
- Bernal SA, Provis JL (2014) Durability of alkali-activated materials: progress and perspectives. *J Am Ceram Soc* 97: 997-1008
- Bernal SA, Provis JL, Rose V, Mejía De Gutierrez R (2011) Evolution of binder structure in sodium silicate-activated slag-metakaolin blends. *Cem Concr Compos* 33: 46-54
- Blackery J, Mitsoulis E (1997) Creeping motion of a sphere in tubes filled with a Bingham plastic material. *J Non-Newtonian Fluid Mech* 70: 59-77
- Boujlel J, Coussot P (2012) Measuring yield stress: a new, practical, and precise technique derived from detailed penetrometry analysis. *Rheol Acta* 51: 867-882
- Chafe NP, de Bruyn JR (2005) Drag and relaxation in a bentonite clay suspension. *J Non-Newtonian Fluid Mech* 131: 44-52

- Chen W, Brouwers HJH (2007) The hydration of slag, part 1: reaction models for alkali-activated slag. *J Mater Sci* 42: 428-443
- Figura BD, Prud'homme RK (2010) Hydrating cement pastes: Novel rheological measurement techniques of the acceleration of gelation. *J Rheol* 54: 1363-1378
- Flatt R, Schober I (2012) Superplasticizers and rheology of concrete. In: Roussel N (ed) *Understanding the rheology of concrete*. Woodhead Publishing in Materials, Cambridge, UK, pp 144-208
- Gauffinet-Garrault S (2012) The rheology of cement during setting. In: Roussel N (ed) *Understanding the rheology of concrete*. Woodhead Publishing in Materials, Cambridge, UK, pp 96-113
- Gueslin B, Talini L, Herzhaft B, Peysson Y, Allain C (2006) Flow induced by a sphere settling in an aging yield-stress fluid. *Phys Fluids* 18: 103101
- Gueslin B, Talini L, Peysson Y (2009) Sphere settling in an aging yield stress fluid: Link between the induced flows and the rheological behavior. *Rheol Acta* 48: 961-970
- Hanehara S, Yamada K (1999) Interaction between cement and chemical admixture from the point of cement hydration, absorption behaviour of admixture, and paste rheology. *Cem Concr Res* 29: 1159-1165
- Jarny S, Roussel N, Le Roy R, Coussot P (2008) Modelling thixotropic behavior of fresh cement pastes from MRI measurements. *Cem Concr Res* 38: 616-623
- Jossic L, Magnin A (2001) Drag and stability of objects in a yield stress fluid. *AIChE J* 47: 2666-2672
- Jupe AC, Wilkinson AP, Funkhouser GP (2012) Simultaneous study of mechanical property development and early hydration chemistry in Portland cement slurries using X-ray diffraction and ultrasound reflection. *Cem Concr Res* 42: 1166-1173
- Kashani A, Provis JL, Qiao GG, van Deventer JSJ (2014) The interrelationship between surface chemistry and rheology in alkali activated slag paste. *Constr Build Mater* 65: 583-591
- Kovler K, Roussel N (2011) Properties of fresh and hardened concrete. *Cem Concr Res* 41: 775-792
- Lootens D, Jousset P, Martinie L, Roussel N, Flatt RJ (2009) Yield stress during setting of cement pastes from penetration tests. *Cem Concr Res* 39: 401-408
- Müller M, Tyrach J, Brunn PO (1999) Rheological characterization of machine-applied plasters. *ZKG Int* 52: 252-259
- Nguyen QD, Boger DV (1983) Yield stress measurement for concentrated suspensions. *J Rheol* 27: 321-349
- Nguyen QD, Boger DV (1985) Direct yield stress measurement with the vane method. *J Rheol* 29: 335-347
- Nguyen QD, Boger DV (1987) Characterization of yield stress fluids with concentric cylinder viscometers. *Rheol Acta* 26: 508-515
- Nguyen QD, Boger DV (1992) Measuring the flow properties of yield stress fluids. *Annu Rev Fluid Mech* 24: 47-88
- Ovarlez G, Mahaut F, Bertrand F, Chateau X (2011) Flows and heterogeneities with a vane tool: Magnetic resonance imaging measurements. *J Rheol* 55: 197-223
- Palacios M, Banfill PFG, Puertas F (2008) Rheology and setting of alkali-activated slag pastes and mortars: Effect of organic admixture. *ACI Mater J* 105: 140-148
- Palacios M, Puertas F (2011) Effectiveness of mixing time on hardened properties of waterglass-activated slag pastes and mortars. *ACI Mater J* 108: 73-78

- Plank J, Hirsch C (2007) Impact of zeta potential of early cement hydration phases on superplasticizer adsorption. *Cem Concr Res* 37: 537-542
- Provis JL, Bernal SA (2014) Geopolymers and related alkali-activated materials. *Annu Rev Mater Res* 44: 299-327
- Richardson IG (1999) The nature of C-S-H in hardened cements. *Cem Concr Res* 29: 1131-1147
- Rossler C, Eberhardt A, Kucerova H, Moser B (2008) Influence of hydration on the fluidity of normal Portland cement pastes. *Cem Concr Res* 38: 897-906
- Sant G, Ferraris CF, Weiss J (2008) Rheological properties of cement pastes: A discussion of structure formation and mechanical property development. *Cem Concr Res* 38: 1286-1296
- Schatzmann M, Bezzola GR, Minor HE, Windhab EJ, Fischer P (2009) Rheometry for large-particulated fluids: Analysis of the ball measuring system and comparison to debris flow rheometry. *Rheol Acta* 48: 715-733
- Standards Australia (2010) General Purpose and Blended Cements (AS3972-2010), Sydney
- Tabuteau H, Coussot P, De Bruyn JR (2007) Drag force on a sphere in steady motion through a yield-stress fluid. *J Rheol* 51: 125-137
- Voigt T, Shah SP (2004) Properties of early-age Portland cement mortar monitored with shear wave reflection method *ACI Mater J* 101: 473-482
- Wang SD, Scrivener KL (1995) Hydration products of alkali activated slag cement. *Cem Concr Res* 25: 561-571
- Williams DA, Saak AW, Jennings HM (1999) The influence of mixing on the rheology of fresh cement paste. *Cem Concr Res* 29: 1491-1496
- Yang M, Jennings HM (1995) Influences of mixing methods on the microstructure and rheological behavior of cement paste. *Adv Cem Based Mater* 2: 70-78
- Zhu L, Sun N, Papadopoulos K, De Kee D (2001) A slotted plate device for measuring static yield stress. *J Rheol* 45: 1105-1122
- Zingg A, Holzer L, Kaech A, Winnefeld F, Pakusch J, Becker S, Gauckler L (2008) The microstructure of dispersed and non-dispersed fresh cement pastes - New insight by cryo-microscopy. *Cem Concr Res* 38: 522-529